Loughborough University

This item was submitted to Loughborough's Research Repository by the author.
Items in Figshare are protected by copyright, with all rights reserved, unless otherwise indicated.

Superconductivity-induced change in magnetic anisotropy in epitaxial ferromagnet-superconductor hybrids with spin-orbit interaction

PLEASE CITE THE PUBLISHED VERSION

https://doi.org/10.1103/physrevb.102.020405

PUBLISHER

American Physical Society (APS)

VERSION

VoR (Version of Record)

PUBLISHER STATEMENT

This paper was accepted for publication in the journal Physical Review B and the definitive published version is available at https://doi.org/10.1103/physrevb.102.020405

LICENCE

CC BY-NC-ND 4.0

REPOSITORY RECORD

González-Ruano, César, Lina G Johnsen, Diego Caso, Coriolan Tiusan, Michel Hehn, Niladri Banerjee, Jacob Linder, and Farkhad G Aliev. 2020. “Superconductivity-induced Change in Magnetic Anisotropy in Epitaxial Ferromagnet-superconductor Hybrids with Spin-orbit Interaction”. Loughborough University. https://hdl.handle.net/2134/12659630.v1.

Rapid Communications

Superconductivity-induced change in magnetic anisotropy in epitaxial ferromagnet-superconductor hybrids with spin-orbit interaction

César González-Ruano,[1] Lina G. Johnsen,[2] Diego Caso,[1] Coriolan Tiusan,[3,4] Michel Hehn,[4] Niladri Banerjee,[5] Jacob Linder,[2] and Farkhad G. Aliev[1,*]

[1]*Departamento Física de la Materia Condensada C-III, Instituto Nicolás Cabrera (INC) and Condensed Matter Physics Institute (IFIMAC), Universidad Autónoma de Madrid, Madrid 28049, Spain*

[2]*Center for Quantum Spintronics, Department of Physics, Norwegian University of Science and Technology, NO-7491 Trondheim, Norway*

[3]*Department of Physics and Chemistry, Center of Superconductivity Spintronics and Surface Science C4S, Technical University of Cluj-Napoca, Cluj-Napoca 400114, Romania*

[4]*Institut Jean Lamour, Nancy Universitè, 54506 Vandoeuvre-les-Nancy Cedex, France*

[5]*Department of Physics, Loughborough University, Epinal Way, Loughborough LE11 3TU, United Kingdom*

(Received 10 March 2020; revised 1 July 2020; accepted 1 July 2020; published 15 July 2020)

The interaction between superconductivity and ferromagnetism in thin film superconductor/ferromagnet heterostructures is usually reflected by a change in superconductivity of the S layer set by the magnetic state of the F layers. Here we report the converse effect: transformation of the magnetocrystalline anisotropy of a single Fe(001) layer, and thus its preferred magnetization orientation, driven by the superconductivity of an underlying V layer through a spin-orbit coupled MgO interface. We attribute this to an additional contribution to the free energy of the ferromagnet arising from the controlled generation of triplet Cooper pairs, which depends on the relative angle between the exchange field of the ferromagnet and the spin-orbit field. This is fundamentally different from the commonly observed magnetic domain modification by Meissner screening or domain wall-vortex interaction, and it offers the ability to fundamentally tune magnetic anisotropies using superconductivity—a key step in designing future cryogenic magnetic memories.

DOI: 10.1103/PhysRevB.102.020405

Superconductivity (S) is usually suppressed in the presence of ferromagnetism (F) [1–5]. For example, in F/S/F spin-valves the transition temperature T_C of the S layer is different for a parallel alignment of the F layer moments compared to an antiparallel alignment [6–9]. Interestingly, for noncollinear alignment of the F layer moments in spin-valves [10–12] or Josephson junctions [13–22], an enhancement in the proximity effect is found due to the generation of long-range triplet Cooper pairs, immune to the pair-breaking exchange field in the F layers. So far, the reciprocal modification of the static properties of the ferromagnet by superconductivity has been limited to restructuring [23] and pinning of magnetic domain walls (DWs) by Meissner screening and vortex-mediated pinning of DWs [24–27].

Modification of the magnetization dynamics in the presence of superconductivity has been studied in [28–36]. Recently, theoretical and experimental results have indicated an underlying role of Rashba spin-orbit coupling (SOC), resulting in an enhancement of the proximity effect and a reduction of the superconducting T_C, along with enhanced spin pumping and Josephson current in systems with a single F layer coupled to Nb through a heavy-metal (Pt) [37–43]. In this context, V/MgO/Fe [44] has been shown to be an effective system to study the effect of SOC in S/F structures with fully epitaxial layers.

At first glance, altering the magnetic order in S/F heterostructures leading to a change in the direction of magnetization appears nontrivial due to the difference in the energy scales associated with the order parameters. The exchange splitting of the spin-bands and the superconducting gap are about 10^3 and 10^1 K, respectively. However, this fundamentally changes if one considers the possibility of controlling the magnetocrystalline anisotropy (MCA) by manipulating the competing anisotropy landscape with superconductivity, since the MCA energy scales are comparable to the superconducting gap energy. Interestingly, emergent triplet superconducting phases in S/SOC/F heterostructures offer the possibility to observe MCA modification of a F layer coupled to a superconductor through a spin-orbit coupled interface, triggered by the superconducting phase [45].

In this paper, we present evidence that cubic in-plane MCA in a V/MgO/Fe(001) system is modified by the superconductivity of V through SOC at the MgO/Fe interface [46]. Our detailed characterization of the coercive fields of the rotated soft Fe(001) and sensing hard (Fe/Co) ferromagnetic layers by the tunneling magnetoresistance effect (TMR) [47] along with numerical simulations dismisses the Meissner screening and DW-vortex interactions as a source of the observed effects.

The magnetic tunnel junction (MTJ) multilayer stacks have been grown by molecular beam epitaxy (MBE) in a chamber with a base pressure of 5×10^{-11} mbar following the procedure described in [48]. The samples were grown on [001]

*farkhad.aliev@uam.es

 ©2020 American Physical Society

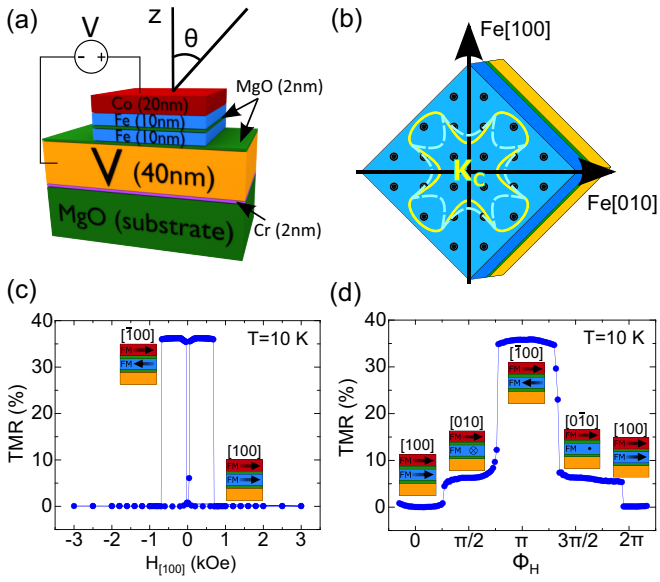


FIG. 1. (a) Sketch of the junctions under study. Fe(10 nm)Co(20 nm) is the hard (sensing) layer while Fe(10 nm) is the soft ferromagnet where spin reorientation transitions are investigated. (b) Sketch showing the top view without the hard Fe/Co layer, with the fourfold in-plane magnetic energy anisotropy expected for the Fe(001) atomic plane of the magnetically free layer, for temperatures above T_C (yellow line) and well below T_C (dashed cyan). Note that during the epitaxial growth, the Fe lattice is rotated by 45° with respect to MgO. Parts (c) and (d) show in-plane spin reorientation transitions between parallel (P), perpendicular in plane (PIP), and antiparallel (AP) relative magnetization alignments of the soft and hard F layers for a 30×30 μm^2 junction at $T = 10$ K (above T_C). Indices above the inset sketches indicate the direction of the soft layer. The in-plane rotation has been carried out with the angle Φ_H of the magnetic field relative to the Fe[100] axis going from $-30°$ to 390°.

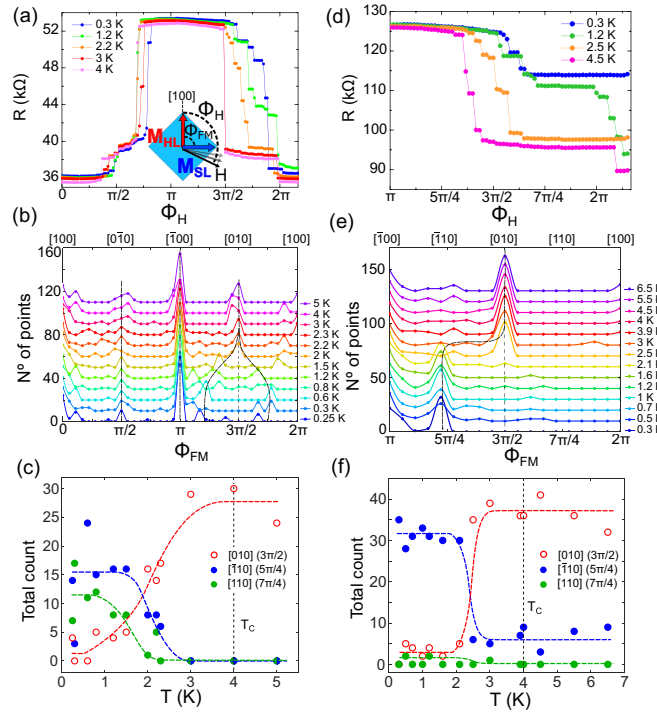


FIG. 2. Typical angular dependence of the resistance of a V/MgO/Fe/MgO/Fe/Co junction on the orientation of the in-plane field with respect to the main crystalline axes from above to below T_C when the rotation is initiated from a P state (a)–(c) and from an AP state (d)–(f). The inset sketches the experimental configuration, showing the angles between the ferromagnetic layers (Φ_{FM}) and of the external magnetic field (Φ_H). Parts (b),(e) correspondingly represent the experimental data shown in (a),(d) in the form of histograms, dividing the 0-2π interval into 36 zones. Parts (c),(f) plot the histograms in (b),(e) as counts vs temperature for the intermediate states (AP + $\pi/4$ or the [1̄10] axis, AP + $\pi/2$ = PIP or [010], and AP + $3\pi/4$ or [110]) for the second half of the rotation.

MgO substrates. Then a 10-nm-thick seed of antidiffusion MgO underlayer is grown on the substrate to trap the C from it before the deposition of the Fe (or V). Then the MgO insulating layer is epitaxially grown by e-beam evaporation, the thickness is approximately ∼2 nm, and so on with the rest of the layers. Each layer is annealed at 450 °C for 20 min for flattening. After the MBE growth, all the MTJ multilayer stacks are patterned in 10–40-μm-sized square junctions (with the diagonal along [100]) by UV lithography and Ar-ion etching, controlled step-by-step *in situ* by Auger spectroscopy. The measurements are performed inside a JANIS® He^3 cryostat. The magnetic field is varied using a three-dimensional (3D) vector magnet. For the in-plane rotations, the magnetic-field magnitude was kept at 70–120 Oe, far away from the soft Fe(001) and hard Fe/Co layer switching fields obtained from in-plane TMRs (see the Supplemental Material S1 and S2 [49], which also incudes Refs. [50–55]). This way, only the soft layer is rotated, and the difference in resistance can be attributed to the angle between the soft and hard layers.

Figure 1(a) shows the device structure with the Fe/Co hard layer sensing the magnetization alignment of the 10-nm-thick Fe(001) soft layer. A typical TMR plot above T_C is shown in Fig. 1(c). The resistance switching shows a standard TMR between the P and AP states. However, the epitaxial Fe(001) has a fourfold in-plane anisotropy with two orthogonal easy axes—[100] and [010]—[Fig. 1(b)]. These MCA states could be accessed by an in-plane rotation of the Fe(001) layer with respect to the Fe/Co layer using a field greater than the coercive field of the Fe(001) layer without disrupting the Fe/Co magnetization (see also the Supplemental Material S1 [49] for the magnetic characterization of the Fe/Co layer). This is shown in Fig. 1(d), where TMR is plotted as a function of the in-plane field angle with respect to the [100] direction angle Φ_H. This gives rise to four distinct magnetization states with P, perpendicular in-plane (PIP), and AP states reflected by the TMR values. Supplemental Material S3 [49] discusses the weak magnetostatic coupling between the two FM layers (detected through resistances in-between the P and AP states in the virgin state of different samples), showing that it does not affect the capability to reorient the soft layer independently of the hard one. It also demonstrates that the soft layer retains different magnetic directions at zero field.

Figure 2 analyzes the most probable in-plane magnetization orientations of the Fe(001) layer through magnetic field rotations at fixed temperatures from above to below T_C. Typically, no qualitative changes in TMR are observed

above and below T_C in the $0-\pi$ field rotation angle (Φ_H) span [Fig. 2(a)]. However, in the $\pi-2\pi$ range, the TMR qualitatively changes below $T_C/2$, possibly indicating new stable magnetization states along different directions from the ones established by the principal crystallographic axes [Fig. 2(a)].

To ascertain the exact angle Φ_{FM} between the two F layers, we have calibrated the magnetization direction of the soft layer with respect to the hard Fe/Co using the Slonczewski formula (Supplemental Material S4 [49]). The applicability of the macrospin approach to describe TMRs and magnetization reorientation resides in the high effective spin polarization obtained ($P = 0.7$) [47], approaching the values typically reported for Fe/MgO in a fully saturated state [56,57]. Figure 2(b) is a histogram representing the probability of obtaining a specific Φ_{FM} as temperature is lowered from above to below T_C. We observe that the most probable Fe(001) directions are oriented along the [100] and [010] principal axes above $T_C/2$, while below $T_C/2$ it splits in three branches roughly oriented along $\pi/4$ angles. The split of the $[0\bar{1}0]$ state into three branches is also visualized in Fig. 2(e), with a plot of the counts versus temperature around the $[\bar{1}10]$, $[0\bar{1}0]$, and $[1\bar{1}0]$ magnetization directions.

Interestingly, once the rotation is initiated in the AP configuration, the magnetization apparently locks in the $(\pi+\pi/4)$ (or $[\bar{1}\bar{1}0]$) state [Figs. 2(b), 2(d) and 2(f)]. This probably arises due to the improved initial macrospin alignment, which is not fully achieved in the AP state with a preceding P-AP rotation. We believe that with the full 2π field rotation, magnetization inhomogeneities or local DWs created during the P-AP state rotation help to overcome MCA energy barriers more easily. The suggested suppression of the local DWs with the magnetization rotation initiated from the AP state can be indirectly inferred from the broadening of the $[\bar{1}00]$ to $[0\bar{1}0]$ transition in the normal state detected as a small (extrinsic) number of counts around $[\bar{1}10]$ [Fig. 2(f)].

For a more systematic analysis, we performed a series of in-plane TMR measurements along different directions relative to the symmetry axes. The first experiment (i) was performed with an initial saturation field of ± 1 kOe in the [100] direction, followed by a TMR in the [210] direction (between [100] and [110]). The second experiment (ii) initially saturates both the hard and soft layers along the [100] direction. Then, a minor loop is performed starting from zero field and going up to 150 Oe along the [110] axis.

Both experiments further suggest the possibility of superconductivity-induced changes of MCA. The inset of Fig. 3(a) shows the full field sweep range in the first (i) configuration, and Fig. 3(a) zooms in close to the AP configuration. When we sweep the field in the [210] direction, we detect a weak but robust resistance upturn at temperatures below approximately $T_C/2$ (Fig. 3). This additional TMR increase [shown by the arrows in Fig. 3(a)] roughly corresponds to an 8–10 degree rotation in the relative spin direction between the soft and hard layer toward their AP alignment (see the Supplemental Material S4 [49] for an analysis of the calculated angle error). Within the proposed macrospin approximation, this could be understood as a redirection of the soft layer magnetization forced by the external field, from the initially blocked [110] direction toward the external

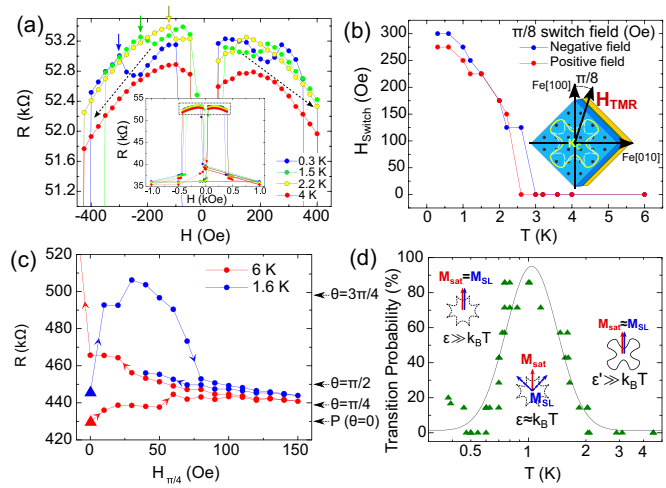


FIG. 3. (a) TMR measurements on an S/F/F 30×30 μm^2 junction with H oriented along [210] [inset in (b)] for various temperatures. The increase in R is associated with a transition from the [110] magnetization orientation to a forced [210] direction of the soft layer. (b) Variation of the transition field with T for the positive and negative field branches. Inset: exchange energy anisotropy and direction of the applied field (H_{TMR}). (c) Two TMRs performed on a 10×10 μm^2 junction in the [110] direction at $T = 6$ and 1.6 K, after applying 1 kOe in the [100] direction. The 6 K TMR starts in a P state, while the 1.6 K TMR starts already in a tilted state. Right axis: estimation of the angle θ between the two F layers based on the Slonczewski formula. (d) Probability of finding a tilted state at $H = 0$ [triangular points in (b)] vs T (in log scale), averaged with seven experimental points around each T. The line is a guide for the eye. Insets: sketch of the magnetic anisotropy below and above T_C, with the saturation magnetization (M_{sat}) and the zero-field magnetization state measured for the soft layer (M_{SL}). ε and ε' represent the energy barrier separating the [100] magnetization direction from the closest minimum below and above T_C, respectively.

field [210] direction. A strong increase of the characteristic field, H_{switch}, required to reorient the soft layer from [110] toward [210] when T decreases below $T_C/2$, could reflect the superconductivity-induced MCA energy minimum along the [110] direction.

The minor TMR loops along [110] [Fig. 3(c)]realized after saturation along [100] point on a thermally induced magnetization reorientation from [100] toward [110] even at zero field, in a temperature range below T_C where the barrier between adjacent energy minima is comparable to k_BT. The zero-field reorientation becomes less probable when the thermal energy is insufficient to overcome the barrier [Fig. 3(d)]. An estimation of the in-plane normal-state MCA energy barrier done through magnetization saturation along [100] and [110] provides a value of only a few μeV/at (Supplemental Material S5 [49]). However, the real barrier is determined by the nucleation volume, which depends on the exchange length in the material. With a DW width of about 3 nm for Fe(001), we estimate the MCA barrier to be at least 10^0–10^1 mV.

Before describing our explanation of the MCA modification of Fe(001) in the superconducting state of the V(40 nm)/MgO(2 nm)/Fe(10 nm) system, we discard alternative

interpretations of the observed effects. Meissner screening [24,25], if present, would introduce about a 10% correction to the actual magnetic field independently of the external field direction (see Supplemental Material S2 [49]). The reason for the weak in-plane field screening could be the small superconductor thickness (40 nm), only slightly exceeding the estimated coherence length (26 nm). On the other hand, intermediate multidomain states are expected to be absent when magnetization is directed along [110] (Supplemental Material S6 [49]). Indeed, our experiments show that magnetization, when locked below T_C in the $(\pi + \pi/4)$ angle, hardly depends on the absolute value of the external field along [110] varied between 0 and 100 Oe. Moreover, simulations of the vortex-DW interaction using MuMax3 [58] and TDGL codes [59] discard the vortex-mediated DW pinning [26,27] scenario including when interfacial magnetic defects created by misfit dislocations [60] are considered (see Supplemental Material S6 [49]). The vortex pinning mechanism also contradicts that only the $(0 - \pi)$ field rotation span [Fig. 2(a)] gets affected below $T_C/2$. The observed irrelevance of the junction area (Supplemental Material S7 [49]) contradicts the importance of the vortex-edge DW interaction. The shape and vortex-DW interaction effects, if relevant, would strengthen magnetization pinning along [100], but not [110] (Supplemental Material S6 and S7 [49]). Finally, we also indicate that the MCA modification from singlet superconductivity would not enable any zero-field rotation to noncollinear misalignment angles, in contrast to our data [Fig. 3(d)].

To explain our results, we consider the possibility in which the invariance of the superconducting proximity effect to magnetization rotation is broken in the presence of SOC. It has been predicted that triplet-superconductivity is effectively generated even for weakly spin-polarized ferromagnets with a small spin-orbit field [61]. In addition to generating triplet pairs, the SOC also introduces an angle-dependent anisotropic depairing field for the triplets [43,45]. In V/MgO/Fe, the Rashba field is caused by a structural broken inversion symmetry at the MgO interfaces [44]. We model our experimental results using a tight-binding Bogoliubov–de Gennes Hamiltonian on a lattice and compute the free energy (Supplemental Material S8 [49]). The Hamiltonian includes electron hopping in and between the different layers, a Rashba-like SOC at the MgO/Fe interface, an exchange splitting between spins in the Fe layers, and conventional s-wave superconductivity in the V layer. The free energy determined from this Hamiltonian includes the contribution from the superconducting proximity effect, and an effective in-plane magnetocrystalline anisotropy favoring magnetization along the [100] and [010] axes. Experimentally, we see a weak antiferromagnetic coupling between the Fe(100) and Fe/Co layers (which does not affect the capability to reorient the soft layer independently of the hard one) described by an additional contribution $f_{AF}\cos(\Phi_{FM})$ with a constant parameter $f_{AF} > 0$.

Figure 4 shows the total free energy of the system as a function of the IP magnetization angle Φ_{FM} for decreasing temperatures. Due to the increase in the superconducting proximity effect, additional local minima appear at $\Phi_{FM} = n\pi/2 + \pi/4$, where $n = 0, 1, 2, \ldots$ (i.e., [110], [$\bar{1}$10], [$\bar{1}\bar{1}$0], and [1$\bar{1}$0], respectively). This is a clear signature for the proximity-induced triplet correlations. These are most efficiently generated at

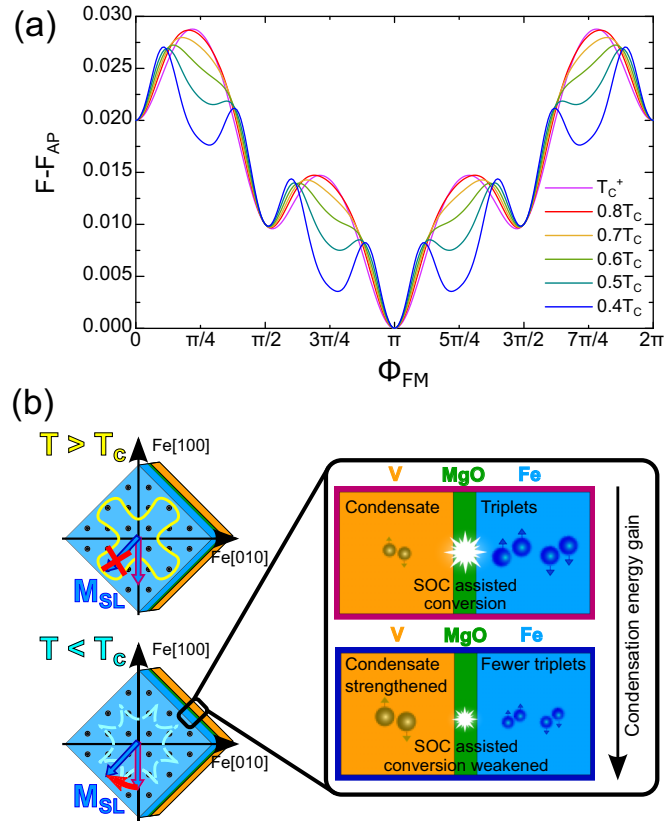


FIG. 4. Numerical modeling. (a) Free energy F vs in-plane magnetization angle Φ_{FM} for temperatures below the superconducting critical temperature and just above the critical temperature (T_C^+). The free energy is plotted relative to the free energy in the AP configuration F_{AP} and has been normalized to the hopping parameter t used in the tight-binding model. (b) Illustration of the physical origin of the change in magnetic anisotropy induced by the superconducting layer. Above T_C, V is a normal metal and the soft Fe layer has a fourfold in-plane magnetic energy anisotropy (yellow line). Below T_C, V is superconducting and influences the soft Fe layer via the proximity effect: a leakage of Cooper pairs into the ferromagnet. Due to the SOC at the interface, a magnetization-orientation-dependent generation of triplet Cooper pairs occurs. The generation of triplets is at its weakest for a magnetization pointing in the [$\bar{1}$10] direction, giving a maximum for the superconducting condensation energy gain. This modifies the magnetic anisotropy of the soft Fe layer (cyan line), enabling magnetization switching to the [$\bar{1}$10] direction (blue arrow). The magnetic anisotropy does not show the weak AP coupling between the two Fe layers, causing an absolute minimum in $\Phi_{FM} = \pi$ (a).

angles $\Phi_{FM} = n\pi/2$ (i.e., [100], [010], [$\bar{1}$00], and [0$\bar{1}$0]) for a heterostructure with a magnetic layer that has a cubic crystal structure like Fe [45]. As a result, the decrease in the free energy is stronger at angles $\Phi_{FM} = n\pi/2 + \pi/4$, where more singlet Cooper pairs survive. Our numerical results thus confirm that the experimentally observed modification of the anisotropy can be explained by the presence of SOC in the S/F structure alone, without including superconducting proximity effects from misalignment between the Fe(100) and Fe/Co layers. Moreover, Fig. 4 illustrates why the $\Phi_{FM} = n\pi/2 + \pi/4$ states only appear experimentally when the external field

is rotated from an AP to P alignment (Fig. 2). Because of the weak AP coupling between the ferromagnetic layers, the energy thresholds for reorienting the magnetization from one local minimum to the next are higher under a rotation from AP to P alignment.

In conclusion, we present experimental evidence for superconductivity-induced change in magnetic anisotropy in epitaxial ferromagnet-superconductor hybrids with spin-orbit interaction. We believe that this mechanism is fundamentally different from the previous reports of magnetization modification arising from Meissner screening and vortex-induced domain wall pinning, even though the spin-triplet mechanism and performed simulations require many assumptions. Our results establish superconductors as tunable sources of magnetic anisotropies and active ingredients for future low dissipation superspintronic technologies. Specifically, they could provide an opportunity to employ spin-orbit proximity effects in magnetic Josephson junction technology and apply it to Fe/MgO-based junctions that are widely used in commercial spintronic applications.

We acknowledge Mairbek Chshiev and Antonio Lara for help with simulations, Yuan Lu for help in sample preparations, and Igor Zutic and Alexandre Buzdin for the discussions. The work in Madrid was supported by Spanish Ministry of Science and Innovation (MAT2015-66000-P, RTI2018-095303-B-C55, EUIN2017-87474) and Consejería de Educación e Investigación de la Comunidad de Madrid (NANOMAGCOST-CM Ref. P2018/NMT-4321) grants. F.G.A. acknowledges financial support from the Spanish Ministry of Science and Innovation, through the María de Maeztu Programme for Units of Excellence in *R&D* (MDM-2014-0377, CEX2018-000805-M). N.B. was supported by EPSRC through the New Investigator Grant EP/S016430/1. The work in Norway was supported by the Research Council of Norway through its Centres of Excellence funding scheme grant 262633 QuSpin. C.T. acknowledges "EMERSPIN" grant ID PN-IIIP4-ID-PCE-2016-0143, No. UEFISCDI: 22/12.07.2017. The work in Nancy was supported by CPER MatDS and the French PIA project "Lorraine Université d'Excellence," reference ANR-15-IDEX-04-LUE.

[1] V. L. Ginzburg, Ferromagnetic superconductors, Zh. Eksp. Teor. Fiz. **31**, 202 (1956) [Sov. Phys. JETP **4**, 153 (1957)].

[2] B. T. Matthias, H. Suhl, and E. Corenzwit, Spin Exchange in Superconductors, Phys. Rev. Lett. **1**, 152 (1958).

[3] A. I. Buzdin, L. N. Bulaevskii, M. L. Kulich, and S. V. Panyukov, Magnetic superconductors, Sov. Phys. Usp. **27**, 927 (1984).

[4] J. Y. Gu, C.-Y. You, J. S. Jiang, J. Pearson, Y. B. Bazaliy, and S. D. Bader, Magnetization-Orientation Dependence of the Superconducting Transition Temperature in the Ferromagnet-Superconductor-Ferromagnet System: CuNi/Nb/CuNi, Phys. Rev. Lett. **89**, 267001 (2002).

[5] I. C. Moraru, W. P. Pratt, Jr., and N. O. Birge, Observation of standard spin-switch effects in ferromagnet/superconductor/ferromagnet trilayers with a strong ferromagnet, Phys. Rev. B **74**, 220507(R) (2006).

[6] L. R. Tagirov, Low-Field Superconducting Spin Switch Based on a Superconductor/Ferromagnet Multilayer, Phys. Rev. Lett. **83**, 2058 (1999).

[7] A. I. Buzdin, A. V. Vedyayev, and N. V. Ryzhanova, Spin-orientation dependent superconductivity in F/S/F structures, Europhys. Lett. **48**, 686 (1999).

[8] I. Baladié, A. Buzdin, N. Ryzhanova, and A. Vedyayev, Interplay of superconductivity and magnetism in superconductor/ferromagnet structures, Phys. Rev. B **63**, 054518 (2001).

[9] P. V. Leksin, N. N. Garif'yanov, I. A. Garifullin, J. Schumann, V. Kataev, O. G. Schmidt, and B. Büchner, Manifestation of New Interference Effects in a Superconductor-Ferromagnet Spin Valve, Phys. Rev. Lett. **106**, 067005 (2011).

[10] X. L. Wang, A. Di Bernardo, N. Banerjee, A. Wells, F. S. Bergeret, M. G. Blamire, and J. W. A. Robinson, Giant triplet proximity effect in superconducting pseudo spin valves with engineered anisotropy, Phys. Rev. B **89**, 140508(R) (2014).

[11] A. Singh, S. Voltan, K. Lahabi, and J. Aarts, Colossal Proximity Effect in a Superconducting Triplet Spin Valve Based on the Half-Metallic Ferromagnet CrO_2, Phys. Rev. X **5**, 021019 (2015).

[12] P. V. Leksin, N. N. Garif'yanov, I. A. Garifullin, Ya. V. Fominov, J. Schumann, Y. Krupskaya, V. Kataev, O. G. Schmidt, and B. Büchner, Evidence for Triplet Superconductivity in a Superconductor-Ferromagnet Spin Valve, Phys. Rev. Lett. **109**, 057005 (2012).

[13] R. S. Keizer, S. T. B. Goennenwein, T. M. Klapwijk, G. Miao, G. Xiao, and A. A. Gupta, A spin triplet supercurrent through the half-metallic ferromagnet CrO_2 , Nature (London) **439**, 825 (2006).

[14] T. S. Khaire, M. A. Khasawneh, W. P. Pratt, Jr., and N. O. Birge, Observation of Spin-Triplet Superconductivity in Co-Based Josephson Junctions, Phys. Rev. Lett. **104**, 137002 (2010).

[15] M. S. Anwar, F. Czeschka, M. Hesselberth, M. Porcu, and J. Aarts, Long-range supercurrents through half-metallic ferromagnetic CrO_2 , Phys. Rev. B **82**, 100501(R) (2010).

[16] J. W. A. Robinson, J. D. S. Witt, and M. G. Blamire, Controlled injection of spin-triplet supercurrents into a strong ferromagnet, Science **329**, 59 (2010).

[17] C. Visani, Z. Sefrioui, J. Tornos, C. Leon, J. Briatico, M. Bibes, A. Barthélémy, J. Santamaría, and J. E. Villegas, Equal-spin Andreev reflection and long-range coherent transport in high-temperature superconductor/halfmetallic ferromagnet junctions, Nat. Phys. **8**, 539 (2012).

[18] N. Banerjee, J. W. A. Robinson, and M. G. Blamire, Reversible control of spin-polarized supercurrents in ferromagnetic Josephson junctions, Nat. Commun. **5**, 4771 (2014).

[19] A. Iovan, T. Golod, and V. M. Krasnov, Controllable generation of a spin-triplet supercurrent in a Josephson spin valve, Phys. Rev. B **90**, 134514 (2014).

[20] J. Linder and J. W. A. Robinson, Superconducting spintronics, Nat. Phys. **11**, 307 (2015).

[21] M. Eschrig, Spin-polarized supercurrents for spintronics: a review of current progress, Rep. Prog. Phys. **78**, 104501 (2015).

[22] M. G. Flokstra, N. Satchell, J. Kim, G. Burnell, P. J. Curran, S. J. Bending, J. F. K. Cooper, C. J. Kinane, S. Langridge, A. Isidori, N. Pugach, M. Eschrig, H. Luetkens, A. Suter, T. Prokscha, and S. L. Lee, Remotely induced magnetism in a normal metal using a superconducting spin-valve, Nat. Phys. **12**, 57 (2016).

[23] A. I. Buzdin and L. N. Bulaevskii, Ferromagnetic film on the surface of a superconductor: Possible onset of inhomogeneous magnetic ordering, Zh. Eksp. Teor. Fiz. **94**, 256 (1988) [Sov. Phys. JETP **67**, 576 (1988)].

[24] L. N. Bulaevskii and E. M. Chudnovsky, Ferromagnetic film on a superconducting substrate, Phys. Rev. B **63**, 012502 (2000).

[25] S. V. Dubonos, A. K. Geim, K. S. Novoselov, and I. V. Grigorieva, Spontaneous magnetization changes and nonlocal effects in mesoscopic ferromagnet-superconductor structures, Phys. Rev. B **65**, 220513R (2002).

[26] J. Fritzsche, R. B. G. Kramer, and V. V. Moshchalkov, Visualization of the vortex-mediated pinning of ferromagnetic domains in superconductor-ferromagnet hybrids, Phys. Rev. B **79**, 132501 (2009).

[27] P. J. Curran *et al.*, Irreversible magnetization switching at the onset of superconductivity in a superconductor ferromagnet hybrid, Appl. Phys. Lett. **107**, 262602 (2015).

[28] X. Weintal and P. W. Brouwer, Magnetic exchange interaction induced by a Josephson current, Phys. Rev. B **65**, 054407 (2002).

[29] Y. Tserkovnyak and A. Brataas, Current and spin torque in double tunnel barrier ferromagnet-superconductor-ferromagnet systems, Phys. Rev. B **65**, 094517 (2002).

[30] C. Bell, S. Milikisyants, M. Huber, and J. Aarts, Spin Dynamics in a Superconductor-Ferromagnet Proximity System, Phys. Rev. Lett. **100**, 047002 (2008).

[31] B. Braude and Ya. M. Blanter, Triplet Josephson Effect with Magnetic Feedback in a Superconductor-Ferromagnet Heterostructure, Phys. Rev. Lett. **100**, 207001 (2008).

[32] E. Zhao and J. A. Sauls, Theory of nonequilibrium spin transport and spin-transfer torque in superconducting-ferromagnetic nanostructures, Phys. Rev. B **78**, 174511 (2008).

[33] F. Konschelle and A. Buzdin, Magnetic Moment Manipulation by a Josephson Current, Phys. Rev. Lett. **102**, 017001 (2019).

[34] J. Linder and T. Yokoyama, Supercurrent-induced magnetization dynamics in a Josephson junction with two misaligned ferromagnetic layers, Phys. Rev. B **83**, 012501 (2011).

[35] J. Linder, A. Brataas, Z. Shomali, and M. Zareyan, Spin-Transfer and Exchange Torques in Ferromagnetic Superconductors, Phys. Rev. Lett. **109**, 237206 (2012).

[36] N. G. Pugach and A. I. Buzdin, Magnetic moment manipulation by triplet Josephson current, Appl. Phys. Lett. **101**, 242602 (2012).

[37] F. S. Bergeret and I. V. Tokatly, Singlet-Triplet Conversion and the Long-Range Proximity Effect in Superconductor-Ferromagnet Structures with Generic Spin Dependent Fields, Phys. Rev. Lett. **110**, 117003 (2013).

[38] N. Banerjee, J. A. Ouassou, Y. Zhu, N. A. Stelmashenko, J. Linder, and M. G. Blamire, Controlling the superconducting transition by spin-orbit coupling, Phys. Rev. B **97**, 184521 (2018).

[39] K.-R. Jeon, C. Ciccarelli, A. J. Ferguson, H. Kurebayashi, L. F. Cohen, X. Montiel, M. Eschrig, J. W. A. Robinson, and M. G. Blamire, Enhanced spin pumping into superconductors provides evidence for superconducting pure spin currents, Nat. Mater. **17**, 499 (2018).

[40] K.-R. Jeon, C. Ciccarelli, A. J. Ferguson, H. Kurebayashi, L. F. Cohen, X. Montiel, M. Eschrig, S. Komori, J. W. A. Robinson, and M. G. Blamire, Exchange-field enhancement of superconducting spin pumping, Phys. Rev. B **99**, 024507 (2019).

[41] N. Satchell and N. O. Birge, Supercurrent in ferromagnetic Josephson junctions with heavy metal interlayers, Phys. Rev. B **97**, 214509 (2018).

[42] N. Satchell, R. Loloee, and N. O. Birge, Supercurrent in ferromagnetic Josephson junctions with heavy-metal interlayers. II. Canted magnetization, Phys. Rev. B **99**, 174519 (2019).

[43] S. H. Jacobsen, J. A. Ouassou, and J. Linder, Critical temperature and tunneling spectroscopy of superconductor-ferromagnet hybrids with intrinsic Rashba-Dresselhaus spin-orbit coupling, Phys. Rev. B **92**, 024510 (2015).

[44] I. Martínez, P. Högl, C. González-Ruano, J. P. Cascales, C. Tiusan, Y. Lu, M. Hehn, A. Matos-Abiague, J. Fabian, I. Zutic, and F. G. Aliev, Interfacial Spin-Orbit Coupling: A Platform for Superconducting Spintronics, Phys. Rev. Appl. **13**, 014030 (2020).

[45] L. G. Johnsen, J. Linder, and N. Banerjee, Magnetization reorientation due to superconducting transition in heavy metal heterostructures, Phys. Rev. B **99**, 134516 (2019).

[46] H. X. Yang, M. Chshiev, and B. Dieny, First-principles investigation of the very large perpendicular magnetic anisotropy at Fe/MgO and Co/MgO interfaces, Phys. Rev. B **84**, 054401 (2011).

[47] I. Martínez, C. Tiusan, M. Hehn, M. Chshiev, and F. G. Aliev, Symmetry broken spin reorientation transition in epitaxial MgO/Fe/MgO layers with competing anisotropies, Sci. Rep. **8**, 9463 (2018).

[48] C. Tiusan, F. Greullet, M. Hehn, F. Montaigne, S. Andrieu, and A. Schuhl, Spin tunneling phenomena in single crystal magnetic tunnel junction systems, J. Phys.: Condens. Matter **19**, 165201 (2007).

[49] See Supplemental Material at http://link.aps.org/supplemental/10.1103/PhysRevB.102.020405 for more details about the magnetic characterization of the samples, the micromagnetic and TDGL simulations, and the theoretical modelling.

[50] E. Jal *et al.*, Interface Fe magnetic moment enhancement in MgO/Fe/MgO trilayers, Appl. Phys. Lett. **107**, 092404 (2015).

[51] P. Blaha, K. Schwarz, F. Tran, R. Laskowski, G. K. H. Madsen, and L. D. Marks, An APW+lo program for calculating the properties of solids, J. Chem. Phys. **152**, 074101 (2020).

[52] A. Manchon, H. C. Koo, J. Nitta, S. M. Frolov, and R. A. Duine, New perspectives for Rashba spin-orbit coupling, Nat. Mater. **14**, 871 (2015).

[53] J. C. Slonczewski, Conductance and exchange coupling of two ferromagnets separated by a tunneling barrier, Phys. Rev. B **39**, 6995 (1989).

[54] A. N. Anisimov, M. Farle, P. Poulopoulos, W. Platow, K. Baberschke, P. Isberg, R. Wäppling, A. M. N. Niklasson, and O. Eriksson, Orbital Magnetism and Magnetic Anisotropy Probed with Ferromagnetic Resonance, Phys. Rev. Lett. **82**, 2390 (1999).

[55] J. Bardeen, L. N. Cooper, and J. R. Schrieffer, Theory of superconductivity, Phys. Rev. **108**, 1175 (1957).

[56] S. S. P. Parkin, C. Kaiser, A. Panchula, P. M. Rice, B. Hughes, M. Samant, and S.-H. Yang, Giant tunneling magnetoresistance at room temperature with MgO (100) tunnel barriers, Nat. Mater. **3**, 862 (2004).

[57] S. Yuasa, T. Nagahama, A. Fukushima, Y. Suzuki, and K. Ando, Giant room temperature magnetoresistance in single-crystal Fe/MgO/Fe magnetic tunnel junctions, Nat. Mater. **3**, 868 (2004).

[58] A. Vansteenkiste, J. Leliaert, M. Dvornik, M. Helsen, F. Garcia-Sanchez, and B. Van Waeyenberge, The design and verification of MuMax3, AIP Adv. **4**, 107133 (2014).

[59] A. Lara, C. González-Ruano, and F. G. Aliev, Time-dependent Ginzburg-Landau simulations of superconducting vortices in three dimensions, Low Temp. Phys. **46**, 316 (2020).

[60] D. Herranz, F. Bonell, A. Gomez-Ibarlucea, S. Andrieu, F. Montaigne, R. Villar, C. Tiusan, and F. G. Aliev, Strongly suppressed 1/f noise and enhanced magnetoresistance in epitaxial Fe-V/MgO/Fe magnetic tunnel junctions, Appl. Phys. Lett. **96**, 202501 (2010).

[61] T. Vezin, C. Shen, J. E. Han, and I. Žutić, Enhanced spin-triplet pairing in magnetic junctions with s-wave superconductors, Phys. Rev. B **101**, 014515 (2020).